DOI: 10.1002/chem.200700247

Highly Reduced, Polyoxo(alkoxo)vanadium(III/IV) Clusters

Ian S. Tidmarsh,[a] Rebecca H. Laye,*[a] Paul R. Brearley,[a] Maheswaran Shanmugam,[a] E. Carolina Sañudo,[a] Lorenzo Sorace,[b] Andrea Caneschi,[b] and Eric J. L. McInnes*[a]

Abstract: A family of high nuclearity oxo(alkoxo)vanadium clusters in unprecedentedly low oxidation states is reported, synthesised from simple vanadium diketonate precursors in alcohols under solvothermal conditions. Crystal structures of $[V_{18}(O)_{12}(OH)_2(H_2O)_4(EtO)_{22}(O_2CPh)_6(acac)_2]$ (**1**), $[V_{16}Na_2(O)_{18}(EtO)_{16}(EtOH)_2(O_2CPh)_6(HO_2CPh)_2]_\infty$ (**2**), $[V_{13}(O)_{13}(EtO)_{15}(EtOH)(RCO_2)_3]$ in which R = adamantyl (**3**) or Ph_3C (**4**), and $[V_{11}(O)_{12}(EtO)_{13}(EtOH)(Ph_3CCO_2)_2(MePO_3)]$ (**5**) are reported, revealing these to be $\{V^{III}_{16}V^{IV}_2\}$ (**1**), $\{V^{III}_9V^{IV}_3V^{V}\}$ (**3** and **4**) and $\{V^{III}_3V^{IV}_8\}$ (**5**) clusters, while **2** consists of isolated $\{V^{III}_8V^{IV}_8\}$ clusters bridged into polymeric chains by $\{Na_2(OEt)_2\}$ fragments. Solvothermal conditions are essential to the formation of these species, and the level of oxidation of the isolated clusters is in part controlled by the crystallisation time, with the lowest mean-oxidation-state species being isolated by direct crystallisation on controlled cooling of the reaction solutions.

Keywords: cluster compounds · polyoxometalates · solvothermal synthesis · vanadium

Introduction

There is a remarkable lack of literature on low-valent vanadium cluster chemistry, in stark contrast to the very mature fields of metal(II/III) clusters of later transition ions,[1] and of high-valent vanadium(IV/V) cluster chemistry in the form of the polyoxo(alkoxo)vanadates.[2,3] The latter species have found much interest for their redox, electrical and magnetic properties, recent examples including Daniel and Hartl's $[V_6O_7(OR)_{12}]^{n+}$ ion, which displays five discrete oxidation states ranging from $\{V^{IV}_2V^{V}_4\}$ to $\{V^{IV}_6\}$,[4] and hybrid conducting materials, such as Coronado's $[BEDT\text{-}TTF]_5[H_3V_{10}O_{28}]$ (BEDT-TTF = bis(ethylenedithio)tetrathiafulvalene).[5] So-called "fully reduced" examples,[6] defined as those that contain only vanadium(IV) ions, have been of particular interest for their magnetic properties,[7] with notable examples including a rare ferromagnetically coupled, large-spin ground-state vanadyl $\{V^{IV}_8\}$ cluster,[8] and Müller's layered $\{V^{IV}_{15}\}$ species,[9] which has been important in studies of spin frustration and phonon bottleneck phenomena. Given these exciting properties it seems a logical step to extend this chemistry to vanadium(III), particularly given the potentially useful properties of this ion[10] for materials such as single-molecule magnets.[11a] However, to the best of our knowledge there are only three reported homovalent tetrametallic V^{III} clusters,[11] and only four larger examples—the cyclic structures $(R_2NH_2)[V_7MF_8(O_2CR)_{16}]$ (M = divalent metal ion),[12] $[V_8(OH)_4(OEt)_8(O_2CR)_{12}]$[13,14] (R = Me, Ph) and $[V_{10}(OMe)_{20}(O_2CMe)_{10}]$.[14] Even for mixed low-valence $V^{III/IV}$ species, there is only one tetrametallic, $\{V^{III}_2V^{IV}_2\}$,[15] and two larger examples, $[Ph_4P]_2[Bu_4N][(V^{IV}O)_6V^{III}\{BuP(O)_2OPO_3\}_6]$[16] and $[V^{III}_2(V^{IV}O)_8(OH)_4(Me_2bta)_8(OMe)_{10}]$ (Me_2btaH = 5,6-dimethylbenzotriazole).[17]

In contrast to the dearth of discrete molecular species, a number of V^{III} and $V^{III/IV}$ extended lattice oxide, phosphate and organophosphate materials are known.[18] Zubieta has suggested that the preference of the V^{III} ion for extended lattices is partly explained by its regular octahedral geometry favouring more extensive connectivity between metal (or heteroatom) centres, in contrast to the highly distorted $\{VO_6\}$ or $\{VO_{4/5}\}$ geometries characteristic of $V^{IV/V}$ due to multiply bonded oxo groups.[19] Nevertheless, the existence of these extended lattices suggests that more molecular clus-

[a] Dr. I. S. Tidmarsh, Dr. R. H. Laye, P. R. Brearley, Dr. M. Shanmugam, Dr. E. C. Sañudo, Prof. E. J. L. McInnes
School of Chemistry, The University of Manchester
Manchester M13 9PL (UK)
Fax: (+44) 161-275-4469
E-mail: Rebecca.H.Laye@manchester.ac.uk
eric.mcinnes@manchester.ac.uk

[b] Dr. L. Sorace, Prof. A. Caneschi
Dipartimento di Chimica, Università di Firenze
and UdR INSTM, Via della Lastruccia 3
Sesto Fiorentino (Italy)

Supporting information for this article is available on the WWW under http://www.chemeurj.org/ or from the author.

ters should be isolable, and the evident explanation for the lack of examples is the easily oxidisable nature of V^{III}, particularly to the stable vanadyl ion, $\{V^{IV}{=}O\}^{2+}$. Therefore, the first challenge in the study of such species is how to prepare them.

Our approach to this problem has been to exploit solvothermal synthetic techniques under reducing conditions in order to stabilise the low oxidation states.[20] Solvo- (specifically, hydro-)thermal techniques have long been used in polyoxovanadate synthesis,[3d,21] and Zubieta has also isolated V^{III}-containing organophosphate extended lattices from V^{IV} reagents in the presence of organoamines as reducing agents.[18b] We have used alcohols as solvents under solvothermal conditions, since this not only provides a reducing environment, but also provides a good source of bridging ligand in the form of alkoxides. [The use of alkoxides has previously been observed to aid isolation of "fully reduced" V^{IV} clusters by reducing the negative charge density cf. "naked" polyoxovanadates.][22] This route led to the $\{V^{III}_8\}$, $\{V^{III}_{10}\}$[14] and $\{V^{III}_2V^{IV}_8\}$[18] clusters above. While the fist two species contain little or no inorganic oxide, the last example is intriguing since it has a 10:12 V/O(H) ratio (including eight vanadyls); hence, this cluster is an example of a polyoxo(alkoxo)vanadium cluster that is more highly reduced than the "fully reduced", all d^1 polyoxo(alkoxo)vanadates.

In this work we report the extension of this chemistry to solvothermal reactions in alcohols of simple vanadium diketonate starting materials to isolate new $\{V^{III}_{16}V^{IV}_2\}$, $\{V^{III}_9V^{IV}_3V^{V}\}$ and $\{V^{III}_3V^{IV}_8\}$ molecular clusters, as well as a $\{V^{III}_8V^{IV}_8\}$ cluster bridged into a polymeric chain by $\{Na_2(OEt)_2\}$ fragments. These species can be considered to derive from simple building blocks, which themselves have analogues (structurally but not in oxidation state) in conventional high-valent polyoxo(alkoxo)metallate chemistry. One of these complexes has appeared in a preliminary communication.[23]

Results

Synthesis and structural studies

*$[V_{18}(O)_{12}(OH)_2(H_2O)_4(EtO)_{22}(O_2CPh)_6(acac)_2]$ (**1**)*: Heating a solution of $[V(acac)_3]$, $[VO(acac)_2]$ ($acac^- =$ acetylacetonate) and $PhCO_2H$ (8:1:3) in EtOH at 150 °C for 12 h under an inert atmosphere, followed by slow cooling, gives brown crystals of **1** direct from the reaction solution (ca. 30 %). Single-crystal X-ray diffraction analysis shows **1** to be $[V_{18}(O)_{12}(OH)_2(H_2O)_4(EtO)_{22}(O_2CPh)_6(acac)_2]$, containing sixteen V^{III} and two V^{IV} ions, the latter present as vanadyl (see below). Hence, **1** can be alternatively formulated as $[V^{III}_{16}(V^{IV}O)_2(O)_{10}(OH)_2(H_2O)_4(EtO)_{22}(O_2CPh)_6(acac)_2]$.

Molecules of **1** are centrosymmetric and the structure can be described as two opened-tetrahedral $\{V^{III}_4\}$ units linked to two square-based pyramidal $\{V^{III}_4V^{IV}\}$ fragments (Figure 1). All vanadium ions have a $\{VO_6\}$ coordination en-

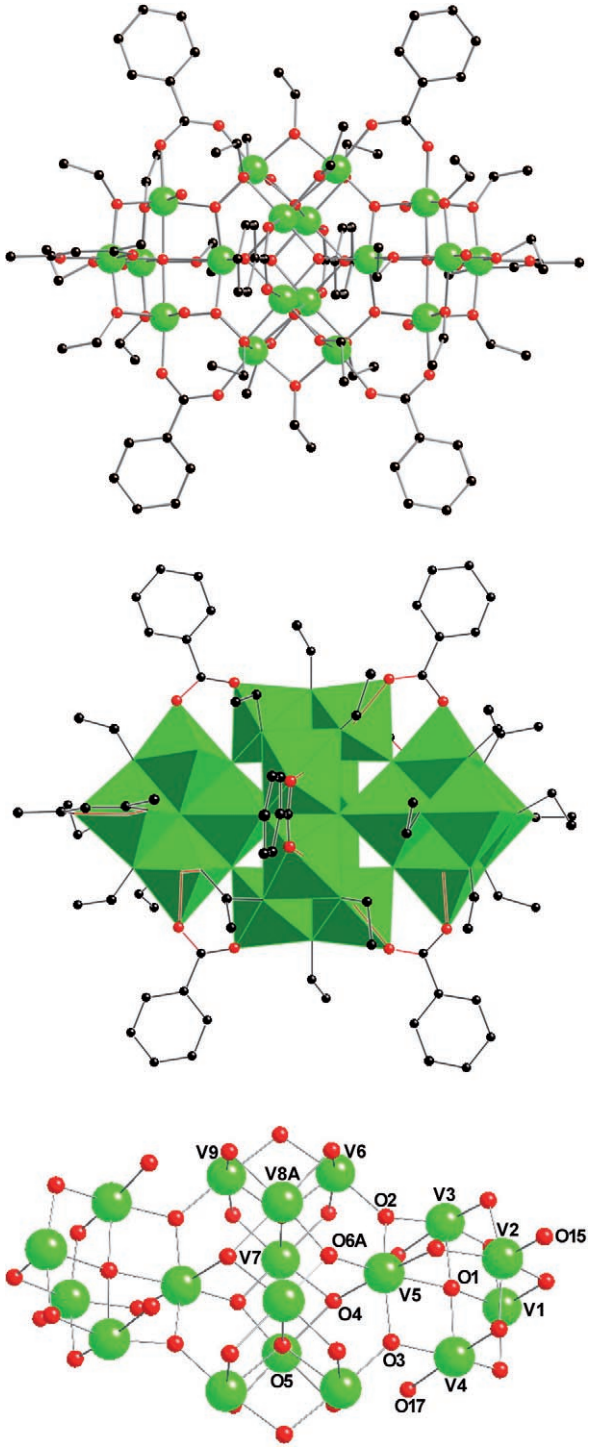

Figure 1. Molecular structure (top), vanadium oxygen core (middle) and $\{VO_6\}$ polyhedral representation (bottom) of $[V^{III}_{16}(V^{IV}O)_2(O)_{10}(OH)_2(H_2O)_4(EtO)_{22}(OCPh)_6(acac)_2]$ (**1**). Selected bond length ranges (Å): V2–O15 1.619(9), V–(μ_4-)O5 1.923(5)–2.015(5), V–(μ_3-)O4(H) 2.092(5)–2.305(5), V–(μ_3-)O6 1.919(5)–1.947(5), V–(μ_5-)O1 2.077(6)–2.191(6), V–(μ_3-)O2,O3 1.871(6)–2.015(5), V–(μ_3-)O6 1.919(5)–1.947(5), V–(μ_3-)O4(H) 2.092(5)–2.305(5), V–O(Et) 1.879(9)–2.098(6), V3,V4–O(H_2) 2.288(9) and 2.291(9), V–O(carboxylate) 2.018(7)–2.044(6). Green (V), red (O), black (C), H omitted for clarity. Atoms labelled "A" indicate atoms at $(1-x, 1-y, 1-z)$.

vironment. The $\{V^{III}_4\}$ units (V6-V7-V8A-V9 and symmetry equivalents (s.e.)) consist of four edge-sharing $\{VO_6\}$ octahedra (Figure 1, bottom), centred on a μ_4-oxide (O5A and s.e.) and bound by five μ_2-ethoxide groups. The V-O5-V angles range from 98.1(2)–102.2(2)° with the exception of 148.9(3)°, which opens the V7-O5A-V8A edge. The two $\{V^{III}_4\}$ units fuse along the O4···O6 and symmetry equivalent edges (also bridged by two μ_2-benzoates) to form an octametallic core. The $\{V^{III}_4V^{IV}\}$ units (V1–V5 and s.e.) consist of five edge-sharing $\{VO_6\}$ octahedra defining a square-based pyramid with V2 at the apex, bound by a μ_5-oxide (O1). Six μ_2-ethoxides span each apex-basal edge of the square-based pyramid and two of the basal edges. V2 and symmetry equivalents have a terminal oxide (V2–O15 1.619(9) Å); these are the only terminal oxides in the structure. One of the basal ions (V1) has a chelating $acac^-$; these are the only diketonates in the structure despite their preponderance in the starting materials, and presumably $acac^-$ is acting as the base for the deprotonation of solvent to provide the 22 bridging alkoxides. V3 and V4 have terminal waters (O16 and O17) at distances of 2.288(9) and 2.291(9) Å, respectively. Cluster **1** is much more air sensitive than **2**–**5** (see below) and we presume this is a consequence of these four V^{III}-bound terminal water molecules, exposing these ions to easy oxidation by loss of protons to form V=O. Clusters **2**–**5** do not contain terminal water molecules.

One basal vanadium ion (V5) in each of the pentametallic units links to the octametallic core through four vertex-sharing interactions (O2, O3, O4 and O6A). The oxygen atoms O2 and O3 are μ_3, lie virtually in their respective V_3O planes and each link one tetrametallic unit (through V6 or V9, respectively) to an edge of a pentametallic unit (V3···V5 or V4···V5, respectively). The oxygen atoms O4 and O6A are also μ_3 and bind both tetrametallic units to V5 or symmetry equivalent. Atom O4 does not lie in the V_3O plane (0.643 Å mean deviation from the plane), and the V–O4 bond lengths (2.092(5)-2.305(5) Å) are significantly longer than V–O2,3,6 (1.871(6)–2.015(5) Å). These longer distances are consistent with protonation of O4 and indeed bond valence sum (BVS) analyses[24] of all these oxide environments indicate that O4 is in fact hydroxide, while O1, O2, O3 and O6 are oxide (see Supporting Information).

Atom V2 and its symmetry equivalent have terminal oxides (O15 and s.e.) at 1.619(9) Å, characteristic of the vanadyl ion (V^{IV}=O). BVS analysis[24] is consistent with this (valence sum 4.00, see Supporting Information for full details), and with the assignment of all the remaining metal ions as V^{III} (mean valence sum 2.91) as expected given their regular octahedral geometry. These assignments are also consistent with charge balance requirements. Six benzoates bridge between the $\{V^{III}_4\}$ and $\{V^{III}_4V^{IV}\}$ fragments: two bind the two $\{V^{III}_4\}$ fragments along the V7···V8 and the symmetry equivalent edge, with a further four connecting the $\{V^{III}_4\}$ and $\{V^{III}_4V^{IV}\}$ fragments along the V3···V6, V4A···V9 and symmetry equivalent edges.

*$[V_{16}Na_2(O)_{18}(EtO)_{16}(EtOH)_2(O_2CPh)_6(HO_2CPh)_2]_\infty$ (**2**)*: A similar reaction to that which gives **1** but in the presence of Na(OEt)—solvothermal heating of $[V(acac)_3]$, $[VO(acac)_2]$, $PhCO_2H$ and Na(OEt) (5:3:4:6)—yields the structurally related coordination polymer $[V_{16}Na_2(O)_{18}(EtO)_{16}(EtOH)_2(O_2CPh)_6(HO_2CPh)_2]_\infty$ (**2**) in approximately 25% yield. Cluster **2** contains eight V^{III} and eight V^{IV} ions, six of which are present as vanadyl, hence it can be formulated as $[V^{III}_8V^{IV}_2(V^{IV}O)_6Na_2(O)_{12}(EtO)_{16}(EtOH)_2(O_2CPh)_6(HO_2CPh)_2]_\infty$.

The repeating vanadium cluster of **2** is centrosymmetric and consists of two opened-tetrahedral $\{V^{III}_4\}$ units linked to two puckered planar (or, alternatively, flattened tetrahedral) $\{V_4\}$ fragments (Figure 2). The $\{V^{III}_4\}$ units (V5–V7,V8A and s.e.) are analogous to those of **1**, together forming an identical octa-metallic core (mean BVS at vanadium, 3.06).

The $\{V_4\}$ units (V1–4 and s.e.) consist of four $\{V^{IV}O_5\}$ polyhedra that edge-share, centred on a compressed tetrahedral μ_4-oxide (O1) and bound by two μ_2-ethoxides (O20, O21) and two μ_3-oxides (O2, O6A). The vanadium ions V1–V4 all have one short V–O distance, indicative of a degree of multiple bond order, and these alternate between pointing above and below the V4 "plane". The vanadium ions V1, V2 and V4 (mean valence sum 4.12) have slightly distorted square-based pyramidal $\{VO_5\}$ geometries with terminal oxides O15, O16 and O17, respectively. Atom V1 has a further long contact to a benzoic acid *trans* to O15 (V1–O8 2.557 Å). Atom V3 (valence sum 3.84) also has a near square-pyramidal $\{VO_5\}$ geometry with O3 at the apex and, although it does not have a terminal oxide, the V3–O3 bond length is short at 1.698(4) Å. Atom V3 links to the octa-metallic core through four vertex-sharing interactions (O2, O3, O4A and O6A, all μ_3-O^{2-} by BVS).

The oxygen atoms O2 and O6A each link one $\{V^{III}_4\}$ unit (through V6 or V7, respectively) to an edge of a $\{V^{IV}_4\}$ unit (V2···V3 or V3···V4, respectively). The oxygen atoms O3 and O4A also bind both $\{V^{III}_4\}$ units to V3. The V^{III}–O3 bond lengths are 2.103(3) and 2.102(3) Å, with the V^{IV}–O3 length significantly shorter at 1.698(3) Å. The same trend is observed for O4A. As with **1**, six benzoates link the $\{V^{III}_4\}$ and $\{V^{IV}_4\}$ fragments to each other.

The $\{V^{III}_8V^{IV}_8\}$ clusters are linked into chains along the crystallographic *c* axis through $\{Na_2(OEt)_2\}$ bridges (Figure 3). The vanadyl oxides O16 and O17 bind to Na1, while a benzoic acid links V1 to Na1 (Na1–O8 2.231(5) Å). The sodium ions Na1 and Na1A are bridged by two μ_2-ethoxides (Na1-O(Et)-Na1A 81.91(16)°). A bound ethanol (O18) molecule completes the octahedral coordination geometry around Na.

*$[V_{13}(O)_{13}(EtO)_{15}(EtOH)(AdCO_2)_3]$ (**3**) and $[V_{13}(O)_{13}(EtO)_{15}(EtOH)(Ph_3CCO_2)_3]$ (**4**)*: Heating $[V(acac)_3]$, $[VO(acac)_2]$ and either adamantyl carboxylic ($AdCO_2H$) or triphenylacetic (Ph_3CCO_2H) acid (9:4:3) at 150°C followed by slow cooling and then standing of the reaction mixtures for a period of weeks gives crystals of **3** (28%) or **4** (11%), respectively. Single-crystal X-ray diffraction analysis reveals them to be

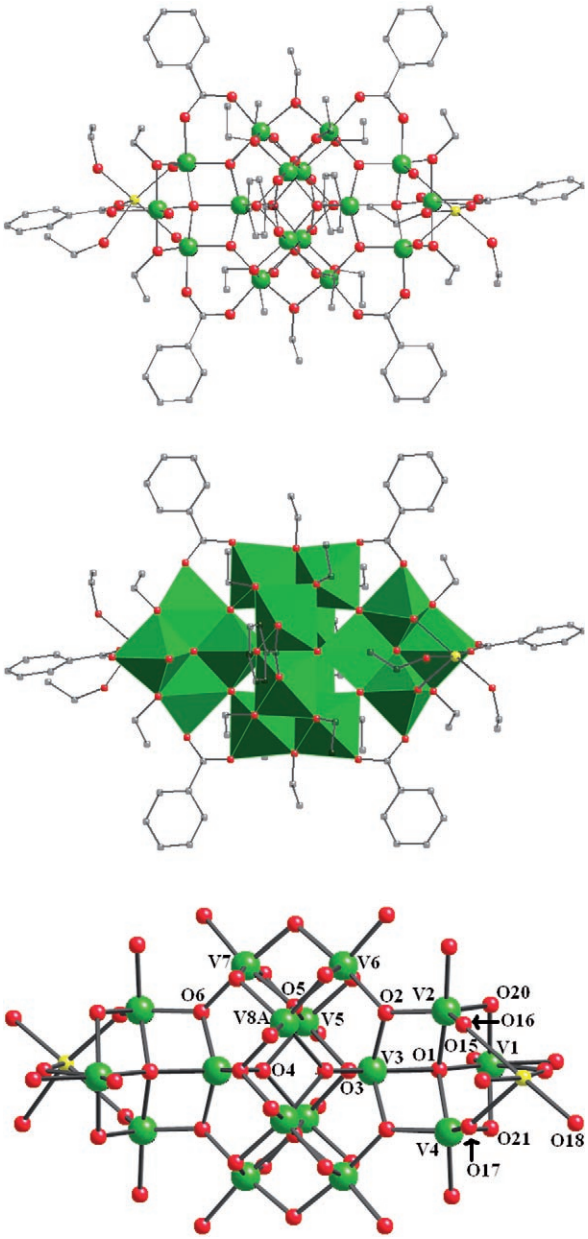

Figure 2. Molecular structure (top), $\{VO_6\}$ and $\{VO_5\}$ polyhedral representation (middle) and vanadium oxide core (bottom) of $[V^{III}{}_8V^{IV}{}_2(V^{IV}O)_6Na_2(O)_{12}(EtO)_{16}(EtOH)_2(OCPh)_6(HOCPh)_2]_\infty$ (**2**). Selected bond length ranges (Å): V–(μ_4-)O5 1.943(5)–1.986(5), V–(μ_4-)O1 1.995(3)–2.055(3), V–(μ_3-)O2,O6 1.858(3)–1.998(3), V1,V2,V4–O15,O16,O17 1.571(4)–1.605(4), Na1–O16,O17 2.479(4) and 2.348(4). Selected angles: *cis* V-O1-V angles 95.44(15)–97.68(15)°, *trans* V-O1-V angles 146.43(18) and V2-O1-V4 133.39(18)°. Colour Scheme as in Figure 1, with Na (yellow).

the tridecametallic species $[V_{13}(O)_{13}(EtO)_{15}(EtOH)(RCO_2)_3]$ [R = Ad (**3**), Ph_3C (**4**)] or, alternatively, $[V^{III}{}_9(V^{IV}O)_3V^{V}(O)_{10}(EtO)_{15}(EtOH)(RCO_2)_3]$.

Complex **3** crystallises in the monoclinic space group $P2_1/n$ and possesses pseudo-threefold symmetry (Figure 4). The structure of **3** can be described in several ways. The vanadium ions V1–V12 can be viewed as consisting of three vertex-sharing $\{V^{III}{}_4V^{IV}\}$ square-based pyramidal fragments

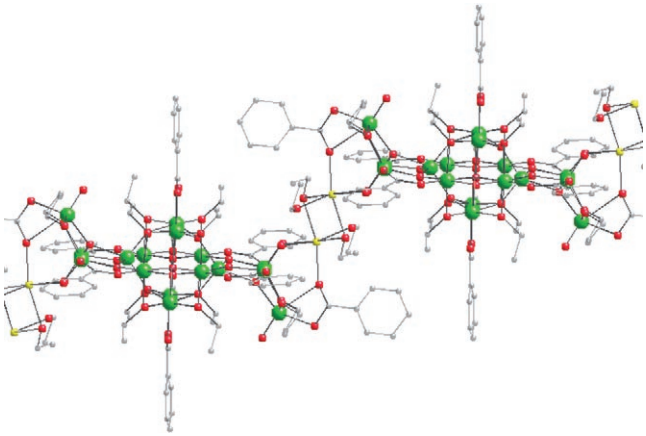

Figure 3. Chains of $[V^{III}{}_8V^{IV}{}_2(V^{IV}O)_6Na_2(O)_{12}(EtO)_{16}(EtOH)_2(OCPh)_6(HOCPh)_2]_\infty$ (**2**) along the crystal *c* axis.

(in which V1, V2 and V6 are the shared vertices), analogous to those in **1**, each centred on a μ_5-oxide and bound by five μ_2-ethoxides, with carboxylates bridging between the fragments analogous to their role in **1** and **2**. The vanadium ions V5, V9 and V12 (all V^{IV} with terminal oxides at 1.661(4)–1.675(5) Å, mean valence sum 3.7) are at the apices of the square-based pyramids, and V1–V4, V6–V8, V10 and V11 (all V^{III}, mean valence sum 3.06) make up the basal planes. The shared vertices V1, V2 and V6 are bound by μ_3-O4, and the three V5, V9 and V12 apices fold away from each other such that V1, V2, V5, V6, V9 and V12 lie on a plane (Figure 5) with the three V^{IV} ions (V5, V9, V12) defining an $\{V^{IV}{}_3V^{III}{}_3\}$ equilateral triangle. Hence, **3** is actually far better described as a layered structure: V3, 4, 7, 8 10, 11 lie on a second, $\{V^{III}{}_6\}$, plane in a distorted hexagon (Figures 5 and 6, top). The two $\{V_6\}$ planes are bridged by three μ_5- and three μ_3-oxides (O1–O3 and O5–O7, respectively) and six μ_2-alkoxides.

A single vanadium ion, V13, makes the third layer in **3** (Figure 5). This is four-coordinate tetrahedral $\{VO_4\}$. Atom V13 is linked to the each member of the $\{V^{III}{}_6\}$ layer by three μ_3-oxides O11–O13 (Figures 4 and 6, top). Atom V13 is V^{V} as indicated by its tetrahedral geometry and short V13–O11,O12,O13 bond lengths (1.690(3)–1.694(3) Å, valence sum 5.21) in contrast to the significantly longer V^{III}–O11,O12,O13 distances (2.090(3)-2.113(3) Å). The coordination at V13 is completed by a terminal EtOH (V13–O14 1.738(4) Å).

A final alternative description of **3** is as four condensed V_3 triangles (V3–V5, V7–V9, V10–V12 (all $V^{III}{}_2V^{IV}$) and V1, V2, V6 ($V^{III}{}_3$)) and a $\{VO_4\}$ unit (Figures 4–6, top).

Complex **4** is analogous to **3**, but with different carboxylate groups; it crystallises in the triclinic $P\bar{1}$ space group such that there are a pair of molecules in the asymmetric unit.

$[V_{11}(O)_{12}(EtO)_{13}(EtOH)(Ph_3CCO_2)_2(MePO_3)]\cdot EtOH$ (***5***): Solvothermal reaction of $[V(acac)_3]$, $[VO(acac)_2]$, Ph_3CCO_2H and methylphosphonic acid $[MeP(O)(OH)_2]$ in a ratio of 9:3:3:3 in EtOH at 150 °C yields $[V_{11}(O)_{12}(EtO)_{13}$-

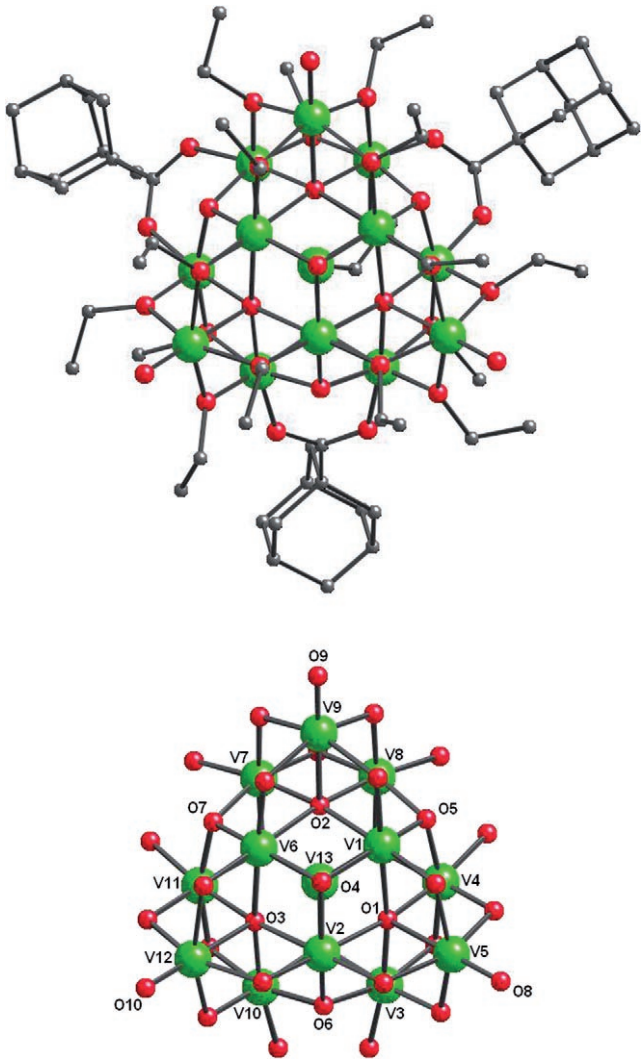

Figure 4. Molecular structure (top) and vanadium oxygen core (bottom) of $[V^{III}_9(V^{IV}O)_3V^{V}(O)_{10}(EtO)_{15}(EtOH)(AdCO_2)_3]$ (**3**). O11, O12 and O13 are eclipsed by V1, V6 and V2, respectively. Selected bond ranges (Å): V^{III}–O1,2,3 2.075(3)–2.174(3), V^{IV}–O2 2.177(3), V–O4 1.888(4)–1.919(7), V–O5,6,7 1.862(4)–1.935(4). Selected inter-bond angle ranges (°): *cis* V-O1,O2,O3-V 88.91(13)–95.40(14), V-O4-V 105.04(16)-06.64(18), V^{III}-O11,O12,O13-V^{III} 92.19(15)–92.80(13), V^{III}–O11,O12,O13–V^{V} 127.16(19)–127.7(2).

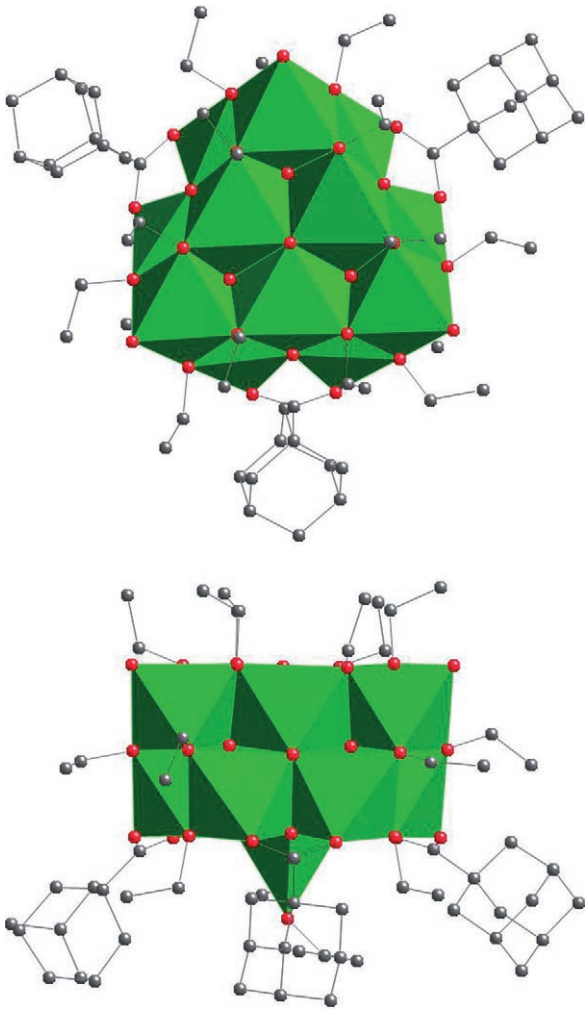

Figure 5. $\{VO_6\}$ and $\{VO_4\}$ polyhedral representation of $[V^{III}_9(V^{IV}O)_3V^{V}(O)_{10}(EtO)_{15}(EtOH)(AdCO_2)_3]$ (**3**) viewed perpendicular to the layers of metal ions (top), with the four coordinate $\{V^{V}O_4\}$ ion to the rear, and within the layers (bottom).

$(EtOH)(Ph_3CCO_2)_2(MePO_3)]\cdot EtOH$ (**5**) or, alternatively, $[V^{III}_3V^{IV}_3(V^{IV}O)_5(O)_7(EtO)_{13}(EtOH)(Ph_3CCO_2)_2(MePO_3)]\cdot EtOH$, in 9% yield after prolonged standing of the cooled solution for several months. Attempts to increase this yield were unsuccessful even when the correct ratio of V^{III} to V^{IV} ions is used.

Complex **5** crystallises in the triclinic space group $P\bar{1}$ with a pair of molecules in the asymmetric unit (labelled **5** and **5′**). The metric parameters are very similar and only **5** will be discussed in detail here. The structure of **5** (Figure 6) is closely related to that of **3**, but with replacement of the $\{(EtOH)V^{V}O_3\}$ component with a doubly deprotonated phosphonate residue $\{MeP(O)_3\}^{2-}$. In addition, one vanadium vertex is missing from the middle $\{V_6\}$ layer of the structure (Figure 7, bottom) and as a consequence the complex is considerably more oxidised than **3** or **4** (see later).

The same layered structure as **3** and **4** is maintained. The vertices of the "top", triangular layer (V5, V9, V11; mean bond valence 3.96) are V^{IV} as before with terminal oxides O8, O9, O12. In contrast to **3** and **4**, the three inner vanadium ions in this layer (V1, V2, V6) are also V^{IV} (mean bond valence 3.90), each having a single short distance to one of the bridging oxides (V1–O4 1.821(10), V2–O6 1.745(10), V6–O7 1.682(9) Å) indicating partial multiple bond order. Atom O4 is significantly asymmetric with respect to the three metal ions as a result. In the "middle" layer of the structure (all V^{III} in **3** and **4**) one of the vanadium vertices is missing with respect to complexes **3** and **4**, leaving an open face in the structure. The vanadium ions neighbouring the missing vertex are now oxidised to V^{IV}, both with terminal oxides (V10–O11, V7–O9; mean valence sum 4.04). The vanadium ions V3, V4 and V8 are the only remaining V^{III} ions in the molecule (mean valence sum 3.01) with similar

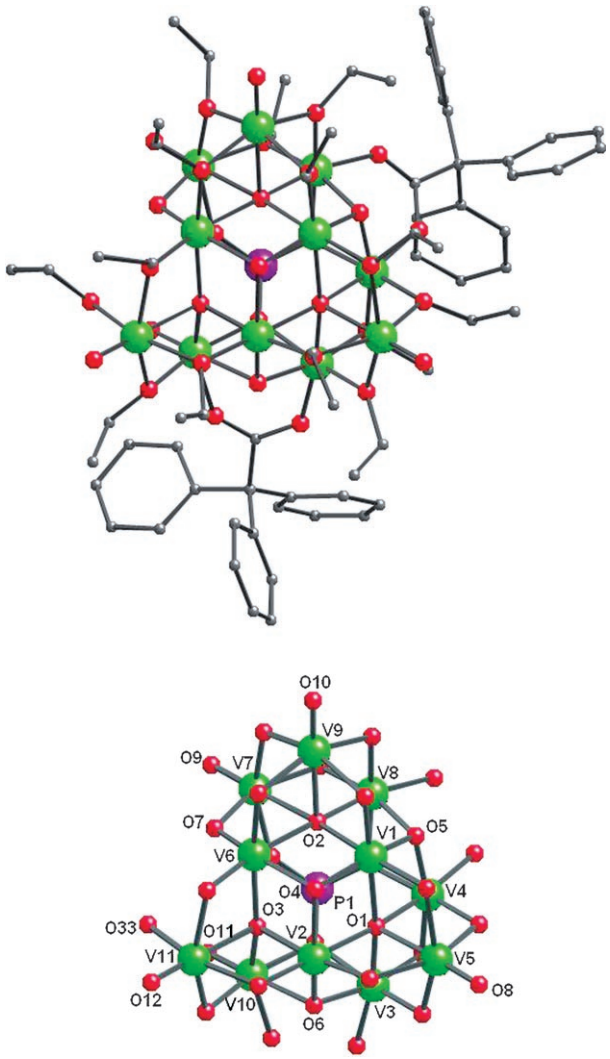

Figure 6. Molecular structure (top) and vanadium oxide core (bottom) of $[V^{III}_3V^{IV}_3(V^{IV}O)_5(O)_7(EtO)_{13}(EtOH)(Ph_3CCO_2)_2(MePO_3)]\cdot EtOH$ (**5**). Selected bond lengths (Å): V5,V9,V11–O8,O9,O12 1.581(11)–1.616(11), V^{III}(V3,V4,V8)–O1,O2 2.024(10)–2.092(9), V^{IV}(V5,V7,V9)–O1,O2 (*trans* to vanadyl) 2.183(9)–2.471(7), V^{IV}(V1,V2,V6)–O1,2 2.116(6)–2.152(10), V–O3 1.958(9)–2.038(9) and 2.198(9) (*trans* to V11,V12), V^{IV}–O(PMe) 2.021(10) and 2.053(10), V^{III}–O(PMe) 2.090(1)–2.131(9).

structural parameters to **3**. The μ_5-oxides O1 and O2 perform the same role as in **3**, while O3 is now only μ_4 due to the "missing" vanadium vertex.

Finally, the tetrahedral vanadium ion of **3** and **4** has been replaced by a doubly deprotonated tetrahedral phosphonate unit which bridges the five vanadium ions by O13–O15 (μ_2, μ_2, μ_1). There are now only two carboxylates, both μ_2, linking V3 and V10, and V4 and V8, analogous to their role in **3** and **4**. There is a carboxylate "missing" (cf. **3** and **4**) at the open face of the cluster, and there is now a terminal EtOH bound at V11 (O33 at 2.001(11) Å).

Magnetic studies: Magnetic susceptibility data for **1**, **2**, **4** and **5** are presented in Figure 8. A full quantitative analysis is not possible at this stage given the size and complexity of

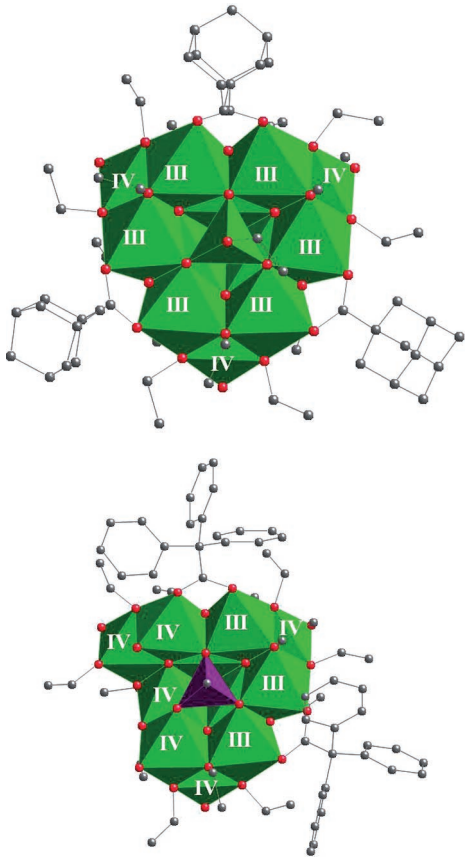

Figure 7. $\{VO_6\}$, $\{VO_4\}$ and $\{PO_3C\}$ polyhedral representation of $[V^{III}_9(V^{IV}O)_3V^{V}(O)_{10}(EtO)_{15}(EtOH)(AdCO_2)_3]$ (**3**) and $[V^{III}_3V^{IV}_3(V^{IV}O)_5(O)_7(EtO)_{13}(EtOH)(Ph_3CCO_2)_2(MePO_3)]$ (**5**) viewed perpendicular to the layers of metal ions, with the four coordinate centre to the front. Colour scheme as in Figure 1 with $\{MePO_3\}$ represented as purple. The oxidation state of the metal ions is indicated in Roman numerals, highlighting the oxidation of the ions at the open face in **5**.

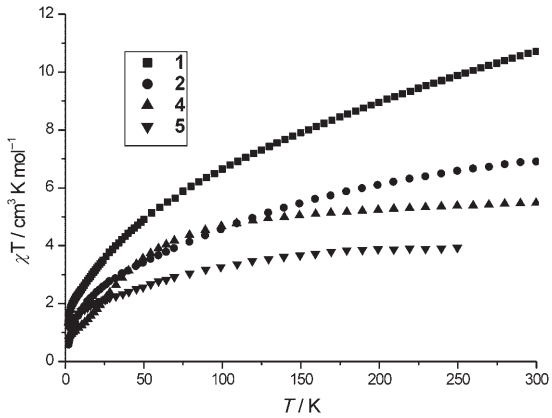

Figure 8. χT versus T plots for **1**, **2**, **4** and **5**.

the spin systems. However, a few qualitative comments can be made. For all clusters χT (χ = molar magnetic susceptibility) decreases with decreasing temperature, indicating dominant antiferromagnetic exchange interactions within the

clusters. In all cases $\chi T(T)$ is still decreasing at base temperature, indicating a small or zero ground-state spin with low-lying excited states that are still populated at the base temperatures. For **1** the room temperature value of χT is 10.7 $cm^3 K mol^{-1}$ and is already decreasing. A plot of χ^{-1} versus T for **1** gives Curie–Weiss behaviour in the high-temperature region (300–150 K) with a Curie constant of 16.8 $cm^3 K mol^{-1}$, which is in excellent agreement with that expected for 16 V^{III} and two V^{IV} uncorrelated spins (16.8 $cm^3 K mol^{-1}$ with $g=2.0$), supporting the assignment of oxidation states. Similar analyses for **2**, **4** and **5** (room temperature χT of 6.7, 5.5 and 3.9 $cm^3 K mol^{-1}$, respectively) give Curie constants of 9.5, 6.0 and 4.3 $cm^3 K mol^{-1}$, respectively. Although these values are significantly smaller than those expected for the uncorrelated spins, the trend (**1** > **2** > **4** > **5**) is consistent with that expected from the oxidation state assignments.

Discussion

We initially isolated the $\{V^{III}_{16}V^{IV}_{2}\}$ cluster **1** by heating a solution of $[V(acac)_3]$ and benzoic acid (4:1) in EtOH at 150 °C for 12 h. This gives crystals of **1** directly on slow cooling of the reaction mixture to room temperature, albeit in low yield (ca. 8 %). The presence of two $\{VO\}^{2+}$ ions in **1** indicates either the presence of an impurity, most likely $[VO(acac)_2]$, in the starting material or serendipitous oxidation of V^{III} during the course of the reaction. The former explanation is favoured by the fact that a much higher yield of **1** (ca. 30 %) is obtained from the post-rationalised reaction stoichiometry of 8:1:3 $[V(acac)_3]/[VO(acac)_2]/PhCO_2H$. Cluster **1** contains 22 ethoxide groups, which derive from the solvent. Hence, in an attempt to increase the yield of this reaction Na(OEt) was added to the reaction mixture. However, the otherwise identical reaction of 8:1:3 $[V(acac)_3]/[VO(acac)_2]/PhCO_2H$ with two equivalents of Na(OEt) instead gives the structurally related coordination polymer **2** in low yield. As with **1**, the yield of this product can be improved dramatically by post-rationalisation of the ratio of reagents—5:3:4:6 gives **2** in approximately 25 % yield.

The structures of **1** and **2** contain common features—they have identical $\{V^{III}_{8}\}$ cores formed from two opened-tetrahedral $\{V^{III}_{4}\}$ fragments. This tetrametallic fragment, formed from four edge-sharing $\{MO_6\}$ polyhedra (Figure 1, bottom), is a common building block in polyoxometallate chemistry—a type **IVb** structural unit in Zubieta's classification.[3] The octametallic core itself is closely related to the known edge-sharing bioctahedral decametallate $\{M_{10}O_{28}\}$ structure[3] with removal of two metal ions from the shared edge. This has been observed previously for Mo in $[Mg_2Mo_8O_{22}(OMe)_6(MeOH)_4]^{2-}$.[25] V5 and V5A have "slipped" away from the $\{V^{III}_{8}\}$ core in **1** (V3 and V3A in **2**) freeing two coordination sites to bridge further to other metal ions. In **1** these secondary fragments are square-based pyramidal $\{V^{III}_{4}V^{IV}\}$ formed from five edge-sharing $\{VO_6\}$ polyhedra (Figure 1, bottom); again this is a known[26] polyoxometallate structural unit (type **V** in Zubieta's classification, derived from the Lindqvist structure).[3] In **2**, these secondary units have oxidised, now consisting of four $\{VO_5\}$ edge-sharing polyhedra forming a puckered, alternating "up and down" $\{V^{IV}_{4}\}$ plane (or very flattened tetrahedron). The Na^+ ions can be considered to have replaced one of the peripheral vanadium ions in **1** and serve to link the clusters into chains (Figure 2). Müller and co-workers have observed similar Na-bridged chains of high-valent polyoxovanadate clusters.[22]

A further common feature of **1** and **2** is that these well-defined $\{V_4\}$ and $\{V_5\}$ structural units are bridged by the carboxylates (Figures 1, bottom, and 2, bottom), between the two $\{V^{III}_{4}\}$ units in both **1** and **2**, and between these units and the secondary $\{V^{III}_{4}V^{IV}\}$ or $\{V^{IV}_{4}\}$ fragments in **1** and **2**, respectively. Therefore, we explored the effect of changing the carboxylic acid in the reaction.

Replacement of benzoic acid in the preparation of **1** with bulkier acids (adamantyl or triphenyl acetic) gives the tridecametallic $\{V^{III}_{9}V^{IV}_{3}V^{V}\}$ species **3** and **4**, rather than the direct analogues of **1**. In contrast to **1**, complexes **3** and **4** only crystallise after standing of the cooled reaction solutions for several weeks. The yields of **3** and **4** can be optimised to 10–30 % by post-rationalisation of the reaction stoichiometry. The $\{V^{III}_{4}V^{IV}\}$ building block of **1** can be identified in the structures of **3** and **4**, with the three carboxylates bridging between them. However, this analogy is probably limited since the three $\{V^{III}_{4}V^{IV}\}$ units share vanadium vertices. Alternatively, it can be considered as four condensed $\{V_3\}$ triangles (themselves formed from three condensed $\{VO_6\}$ polyhedra)—Müller has recently highlighted the importance of this building block in polyoxo(alkoxo)vanadates[22]—with a tetrahedral $\{VO_4\}$ unit (Figures 5 and 6, top). This description has some similarities with a Keggin ion, consisting of the same building blocks, but with one of the $\{V_3\}$ triangular faces pushed towards the cluster centre and the tetrahedral $\{VO_4\}$ unit pulled out from the cluster centre. However, the cluster is probably best described as layered with $\{V^{III}_{3}V^{IV}_{3}\}$, $\{V^{III}_{6}\}$ and $\{V^{V}\}$ layers (Figure 5).

Given the crude similarity between the structures of **3** and **4** and a Keggin ion in terms of the building blocks, we attempted to replace the $\{V^{V}O_4\}$ unit with a tetrahedral main group fragment. Indeed, solvothermal reaction of $[V(acac)_3]$, $[VO(acac)_2]$, Ph_3CCO_2H and $[MeP(O)(OH)_2]$ gives the $\{V^{III}_{3}V^{IV}_{8}P\}$ cluster **5**, in which the phosphonate has substituted for $\{VO_4\}$. It is not clear why there is a missing vertex in the middle layer of the structure, but an important consequence is that there is much more extensive oxidation of the cluster, particularly of those ions at the open face (Figures 6 and 7). Crystals of **5** are only obtained in low yield and only after prolonged standing (a period of months) of the reaction mixture after cooling.

Conclusions

We have isolated a family of low-valent oxo-(alkoxo)vanadium(III/IV) clusters that include $\{V^{III}{}_{16}V^{IV}{}_{2}\}$ (**1**), $\{V^{III}{}_{9}V^{IV}{}_{3}V^{V}\}$ (**3** and **4**) and $\{V^{III}{}_{3}V^{IV}{}_{8}\}$ (**5**), as well as a $\{V^{III}{}_{8}V^{IV}{}_{8}\}$ cluster bridged into a polymeric chain by diamagnetic $\{Na_2(OEt)_2\}$ fragments (**2**). These are by far the largest low-valent vanadium clusters reported to date, having mean oxidation states of $V^{3.1+}$ (**1**), $V^{3.5+}$ (**2**), $V^{3.4+}$ (**3**,**4**) and $V^{3.7+}$ (**5**). This was possible by the combined use of solvothermal conditions and alcohols as solvent. All clusters **1**–**5** contain a large number of alkoxides, further emphasizing the role of this bridging unit in stabilizing lower valent vanadium clusters.[3d] However, the carboxylates also play a key role; analogous reactions in the absence of a source of carboxylate do not give any isolable products, and presumably polymeric metal alkoxides are formed. Solvothermal conditions are essential; we failed to isolate any of **1**–**5** from analogous reactions at room temperature or even under reflux. Even though **3**–**5** do not crystallise directly from controlled cooling of the solvothermally heated reaction solutions, these fail to crystallise if the initial reaction is not performed solvothermally.

The crystallisation stage appears to be vital in determining the level of oxidation of the clusters isolated. The least oxidised cluster, **1**, crystallises directly on controlled cooling of the reaction solution, and is almost entirely V^{III} (mean oxidation state $V^{3.1+}$). Clusters **3** and **4** (mean oxidation state $V^{3.4+}$) crystallise only after standing of the solutions for a period of weeks, while **5** (mean oxidation state $V^{3.7+}$) requires months to crystallise. Presumably it is this standing time that gives the opportunity for more extensive oxidation of vanadium in solution, reflected by the mean oxidation state. The crystallisation time seems to be related to the nature of the carboxylate—the much bulkier, more soluble carboxylic acids in **3**–**5** presumably result in more soluble reaction intermediates, leading both to different products and to slower crystallisation.

All of **1**–**5** contain a high proportion of inorganic oxide (i.e. O^{2-}, OH^-, OH_2, and neglecting the bridging alkoxides and carboxylates), with close to 1:1 ratios of V/O [$\{V_{18}O_{12}(OH)_2(OH_2)_4\}$ (**1**), $\{V_{16}O_{18}\}$ (**2**), $\{V_{13}O_{13}\}$ (**3** and **4**) and $\{V_{11}O_{12}\}$ (**5**)]. Thus, we propose that they are well described as new members of the family of the known polyoxo(alkoxo)vanadates, but represent a new branch of this family existing in highly reduced states.

Experimental Section

Synthesis: All manipulations were conducted under anaerobic conditions (dinitrogen purged glove box and argon served Schlenk line). Ethanol was dried by refluxing over iodine-activated magnesium turnings. All of the crystalline products **1**–**5** were isolated from brown solutions, which sometimes also contained a small amount of insoluble and amorphous brown powder, presumably vanadium oxides.

$[V_{18}(O)_{12}(OH)_2(H_2O)_4(EtO)_{22}(OCPh)_6(acac)_2]$ (1): $[V(acac)_3]$ (0.25 g, 0.72 mmol), $[VO(acac)_2]$ (0.024 g, 0.09 mmol), $PhCO_2H$ (0.033 g, 0.27 mmol) and EtOH (9 mL) were heated at 150 °C in a Teflon-lined autoclave for 12 h followed by slow cooling to room temperature to yield brown, plate-like crystals of **1** that were separated by decanting, washed with EtOH and dried in a stream of argon (ca. 30 %). Selected IR data (KBr): $\tilde{\nu}$ = 2923.56 (w), 1596.17 (s), 1557.08 (s), 1415.09 (s), 1100.78 (s), 1058.37 (s), 969.96 (w), 898.37(w), 717.05 (s), 597.26 cm^{-1} (s); elemental analysis calcd (%) for $C_{96}H_{164}O_{56}V_{18}$: C 36.82, H 5.28, V 29.28; found: C 37.38 , H 5.22 , V 29.03.

$[V_{16}Na_2(O)_{18}(EtO)_{16}(EtOH)_2(O_2CPh)_6(HO_2CPh)_2]_\infty$ (2): $[V(acac)_3]$ (0.150 g, 0.43 mmol), $[VO(acac)_2]$ (0.069 g, 0.26 mmol), $PhCO_2H$ (0.042 g, 0.34 mmol), [NaOEt] (0.018 g, 0.26 mmol) and EtOH (9 mL) were treated similarly to the procedure given for **1** to give brown, plate-like crystals of **2** (ca. 26 %). Elemental analysis calcd (%) for $C_{92}H_{134}O_{52}Na_2V_{16}$: C 37.67, H 4.60, Na 1.57, V 27.79; found: C 36.86 , H 4.35 , Na 1.65, V 27.76.

$[V_{13}(O)_{13}(EtO)_{15}(EtOH)(AdCO_2)_3]$ (3): $[V(acac)_3]$ (0.25 g, 0.72 mmol), $[VO(acac)_2]$ (0.085 g, 0.32 mmol), $AdCO_2H$ (0.043 g, 0.24 mmol) and EtOH (9 mL) were treated similarly to the procedure given for **1**. Brown, block-like crystals of **3** (ca. 11 %) grew from the solution over a number of months. Selected IR data (KBr): $\tilde{\nu}$ = 3466.44, 2920.85, 1522.94, 1408.02, 1095.70, 1057.14, 971.09, 840.67, 677.92, 593.61 cm^{-1}; elemental analysis calcd (%) for $C_{65}H_{126}O_{35}V_{13}$: C 36.65, H 7.111, V 31.09; found: C 36.05, H 6.14, V 31.71.

$[V_{13}(O)_{13}(O)_{10}(EtO)_{15}(EtOH)(Ph_3C_2O_2)_3]$ (4): $[V(acac)_3]$ (0.25 g, 0.72 mmol), $[VO(acac)_2]$ (0.085 g, 0.32 mmol), Ph_3CCO_2H (0.069 g, 0.24 mmol) and EtOH (9 mL) were treated similarly to the procedure given for **1**. Brown, needle-like crystals of **4** (ca. 28 %) grew from the solution over a number of weeks. Selected IR data (KBr): $\tilde{\nu}$ = 3448.51, 2924.79, 1546.38, 1376.08, 1093.92, 970.42, 736.49, 698.69, 605.93 cm^{-1}; elemental analysis calcd (%) for $C_{92}H_{126}O_{35}V_{13}$: C 45.02, H 5.17, V 26.98; found: C 44.46, H 5.36, V 26.85.

$[V_{11}(O)_{12}(EtO)_{13}(EtOH)(Ph_3C_2O_2)_2(PO_3Me)]\cdot EtOH$ (5): $[V(acac)_3]$ (0.25 g, 0.72 mmol), $[VO(acac)_2]$ (0.063 g, 0.24 mmol), Ph_3CCO_2H (0.069 g, 0.24 mmol), MeP(O)(OH)2 (0.023 g, 0.24 mmol) and EtOH (9 mL) were treated similarly to the procedure given for **1**. Brown, plate-like crystals of **5** (ca. 9 %) grew from the solution over a number of months. Selected IR data (KBr): $\tilde{\nu}$ = 3448.14, 2923.75, 1554.99, 1377.70, 1095.30, 1041.26, 970.46, 894.11, 698.53, 581.07 cm^{-1}; elemental analysis calcd (%) for $C_{71}H_{109}O_{34}PV_{11}$: C 40.65, H 5.24, P 1.48; found: C 41.51, H 6.28, P 1.87.

Assignment of oxidation states: Unfortunately, **1**–**5** are either insoluble or unstable in solution, thus preventing direct determination of mean oxidation states by redox titration methods. Hence, assignment of oxidation states has been on the basis of bond valence sum calculations[24] and charge balance. Full results of the BVS analyses are in Supporting Information. The coordination chemistry of vanadium is particularly characteristic of its oxidation states since V^{III} favours regular octahedral $\{VO_6\}$ geometry, while V^{IV} and V^{V} form highly distorted $\{VO_6\}$, square-pyramidal or trigonal-bipyramidal $\{VO_5\}$, or tetrahedral $\{VO_4\}$ geometries due to multiply bonded oxo groups.[19] As there are no counterions in the crystal structures, the only real ambiguity regarding charge balance arises from the protonation states of the oxides in the structures. These have also been assessed by BVS methods (see Supporting Information), and only in **1** are some of these found to involve any level of protonation. Even if some the "naked" oxides in **1**–**5** were protonated, this would require lower vanadium oxidation states to satisfy charge balance.

X-ray crystallography: Single-crystal X-ray diffraction data were measured on Bruker SMART 1 K CCD (**3**) and Oxford Diffraction XCalibur2 (**1**, **2**, **4** and **5**) diffractometers. Unit cell details are given in Table 1, and full tables of structural parameters are given in Supporting Information. Selected parameters or ranges are given in the text and figure captions. Structural solution and refinement were preformed with SHELXTL.[27] The structures were solved by direct methods. Refinement of *F2* was against all reflections. All non-hydrogen atoms were refined anisotropically except for those of disordered atoms in **4**, which were left isotropic to preserve the data-to-parameter ratio. Hydrogen atoms were added in geometrically calculated positions except for the hydroxide (O4) and water protons (O16, O17) in **1**, the carboxylic acid protons in **2**

Table 1. Crystallographic details for **1–5**.

	1	**2**	**3**	**4**	**5**
formula	$C_{96}H_{164}O_{56}V_{18}$	$C_{92}H_{134}O_{52}Na_2V_{18}$	$C_{65}H_{126}O_{35}V_{13}$	$C_{92}H_{126}O_{35}V_{13}$	$C_{71}H_{109}O_{34}V_{11}$
M_r	3131.19	2933.01	2129.88	2454.15	2097.89
crystal size [mm]	0.39x0.23x0.03	0.18x0.12x0.04	0.10x0.10x0.05	0.40x0.22x0.13	0.38x0.24x0.03
crystal system	triclinic	triclinic	monoclinic	triclinic	triclinic
space group	$P\bar{1}$	$P\bar{1}$	$P2_1/n$	$P\bar{1}$	$P\bar{1}$
a [Å]	14.0361(13)	13.6973(9)	14.8094(6)	14.7862(16)	14.2988(6)
b [Å]	16.0288(13)	14.6672(10)	22.0783(9)	27.784(3)	23.0484(13)
c [Å]	16.2151(12)	16.6194(12)	27.1619(11)	28.623(3)	28.2692(13)
α [°]	74.367(7)	96.358(6)	90	113.370(14)	71.995(5)
β [°]	87.552(7)	90.326(6)	90.1750(10)	104.636(9)	89.688(4)
γ [°]	65.633(9)	114.511(6)	90	93.319(9)	89.092(4)
V [Å^3]	3190.4(5)	3014.4(4)	8881.0(6)	10277(2)	8859.2(7)
Z	1	1	4	4	4
ρ_{calcd}	1.630	1.616	1.593	1.586	1.573
T [K]	100	100	100	100	100
$2\theta_{max}$ [°]	64.0352	63.9218	49.24	56.4686	63.7952
data collected (unique)	15920 (7765)	17230 (8568)	36015 (10804)	67225 (25081)	44765 (21494)
data used [$I>2\sigma(I)$]	4785	5307	6916	14008	14779
parameters	845	811	1033	2383	2099
$R(F)$	0.0902	0.0445	0.0459	0.0819	0.1075
$wR2$	0.2386	0.1075	0.1101	0.2043	0.2666
$\Delta\rho_{min}$ [e Å^{-3}]	−0.0857	−0.425	−0.399	−0.779	−1.067
$\Delta\rho_{max}$ [e Å^{-3}]	1.330	1.084	0.666	1.606	2.229

(O7), the bound ethanol protons in **3**, **4** (O14) and **5** (O33), none of which were found from the data and were therefore omitted from the refinement.

Some of the structures required substantial modelling to resolve disorder. In particular, for **5** the final R and $wR2$ values are higher than would usually be acceptable, resulting from a lack of data at higher resolutions.

CCDC 299653 (**1**) and 636594–636597 (**2**–**5**) contain the supplementary crystallographic data for this paper. These data can be obtained free of charge from the Cambridge Crystallographic Data Centre via www.ccdc.cam.ac.uk/data_request/cif.

Magnetic measurements: Variable-temperature magnetic data were measured with a Cryogenic S600 SQUID magnetometer on polycrystalline samples at 1 (300–35 K) and 0.1 T (<35 K). The data were corrected for the contribution of the sample holder and for the diamagnetism of the sample estimated from Pascal's constants.

Acknowledgements

We thank Dr Laurent Lisnard (Manchester) for helpful discussions, CCLRC Daresbury Laboratories for access to their synchrotron X-ray sources, the EPSRC, the Leverhulme Trust, the EC (HPRN-CT-1999-00012/TMR network "Molnanomag", and MRTN-CT-2003-504880 "QuEMolNa") for funding.

[1] R. E. P. Winpenny, *Adv. Inorg. Chem.* **2001**, *52*, 1.
[2] For a recent review of polyoxometallate chemistry, including polyoxovanadates, see D.-L. Long, E. Burkholder, L. Cronin, *Chem. Soc. Rev.* **2007**, *36*, 105.
[3] For more expansive reviews on polyoxo- and oxo(alkoxo)vanadates specifically, see: a) M. T. Pope, A. Müller, *Angew. Chem.* **1991**, *103*, 56; *Angew. Chem. Int. Ed. Engl.* **1991**, *30*, 34; b) Q. Chen, J. Zubieta, *Coord. Chem. Rev.* **1992**, *114*, 107; c) J. Zubieta, *Mol. Eng.* **1993**, *3*, 93; d) M. I. Khan, J. Zubieta, *Prog. Inorg. Chem.* **1995**, *43*, 1.
[4] C. Daniel, H. Hartl, *J. Am. Chem. Soc.* **2005**, *127*, 13987.
[5] E. Coronado, J. R. Galán-Mascarós, C. Giménez-Saiz, C. J. Gómez-Garcia, E. Martínez-Ferrero, M. Almeida, E. P. Lopez, *Adv. Mater.* **2004**, *16*, 324.
[6] M. I. Khan, Q. Chen, D. P. Goshorn, J. Zubieta, *Inorg. Chem.* **1993**, *32*, 672.
[7] For a general review of magnetic properties of polyoxometallates, see: A. Müller, F. Peters, M. T. Pope, D. Gatteschi, *Chem. Rev.* **1998**, *98*, 239.
[8] K. Hegetschweiler, B. Morgenstern, J. Zubieta, P. J. Hagrman, N. Lima, R. Sessoli, F. Totti, *Angew. Chem.* **2004**, *116*, 3518; *Angew. Chem. Int. Ed.* **2004**, *43*, 3436; .
[9] D. Gatteschi, L. Pardi, A-L. Barra, A. Müller, J. Doring, *Nature* **1991**, *354*, 463; I. Chiorescu, W. Wernsdorfer, A. Müller, H. Bögge, B. Barbara, *J. Magn. Magn. Mater.* **2000**, *221*, 103.
[10] a) H. Weihe, H. U. Güdel, *J. Am. Chem. Soc.* **1998**, *120*, 2870; b) P. Knopp, K. Wieghardt, B. Nuber, J. Weiss, W. S. Sheldrick, *Inorg. Chem.* **1990**, *29*, 363; c) P. L. W. Treggena-Piggott, H. Weihe, J. Bendix, A.-L. Barra, H. U. Güdel, *Inorg. Chem.* **1999**, *38*, 5928.
[11] a) S. L. Castro, Z. Sun, C. M. Grant, J. C. Bollinger, D. N. Hendrickson, G. Christou, *J. Am. Chem. Soc.* **1998**, *120*, 2365; b) I. S. Lee, J. R. Long, *Dalton Trans.* **2004**, 3434; c) F. H. Fry, B. A. Dougan, N. McCann, C. J. Ziegler, N. E. Brasch, *Inorg. Chem.* **2005**, *44*, 5197.
[12] R. H. Laye, F. K. Larsen, J. Overgaard, C. A. Muryn, E. J. L. McInnes, E. Rentschler, V. Sanchez, S. J. Teat, H. U. Güdel, O. Waldmann, G. A. Timco, R. E. P. Winpenny, *Chem. Commun.* **2005**, 1125.
[13] H. Kumagai, S. Kitagawa, *Chem. Lett.* **1996**, 471.
[14] R. H. Laye, M. Murrie, S. Ochsenbein, A. R. Bell, S. Teat, J. Raftery, H. U. Güdel, E. J. L. McInnes, *Chem. Eur. J.* **2003**, *9*, 6215.
[15] M. Mikuriya, T. Kotera, F. Adachi, S. Bandow, *Chem. Lett.* **1993**, 945.
[16] J. Salta, J. Zubieta, *J. Cluster Sci.* **1996**, *7*, 531.
[17] R. H. Laye, Q. Wei, P. V. Mason, M. Shanmugan, S. J. Teat, E. K. Brechin, D. Collison, E. J. L. McInnes, *J. Am. Chem. Soc.* **2006**, *128*, 9020.
[18] For example: a) R. C. Haushalter, Z. Wang, M. E. Thompson, J. Zubieta, *Inorg. Chem.* **1993**, *32*, 3700; b) V. Soghomonian, R. C. Haushalter, J. Zubieta, *Chem. Mater.* **1995**, *7*, 1648; c) G. Bonavia, R. C. Haushalter, J. Zubieta, *J. Solid State Chem.* **1996**, *126*, 292; d) K. Barthelet, D. Riou, G. Férey, *Chem. Commun.* **2002**, 1492.
[19] R. C. Finn, J. Zubieta, R. C. Haushalter, *Prog. Inorg. Chem.* **2003**, *51*, 421.
[20] R. H. Laye, E. J. L. McInnes, *Eur. J. Inorg. Chem.* **2004**, 2811.

[21] a) J. Livage, *Coord. Chem. Rev.* **1998**, *178–180*, 999; b) J. Do, R. P. Bontchev, A. J. Jacobsen, *Inorg. Chem.* **2000**, *39*, 3230.
[22] A. Müller, J. Meyer, H. Bogge, A. Stammler, A. Botar, *Chem. Eur. J.* **1998**, *4*, 1388.
[23] I. S. Tidmarsh, R. H. Laye, P. R. Brearley, M. Shanmugan, E. C. Sañudo, L. Sorace, A. Caneschi, E. J. L. McInnes, *Chem. Commun.* **2006**, 2560.
[24] a) I. D. Brown, R. D. Shannon, *Acta. Crystallogr. Sect. A* **1973**, *29*, 266; b) I. D. Brown, K. K. Woo, *Acta Crystallogr. Sect. B* **1976**, *32*, 1957; c) W. Liu, H. H. Thorp, *Inorg. Chem.* **1993**, *32*, 4102.
[25] M. Yu. Antipin, L. P. Didenko, L. M. Kachapina, A. E. Shilov, A. K. Shiolva, Y. T. Struchkov, *J. Chem. Soc. Chem. Commun.* **1989**, 1467.
[26] P. Gouzerh, Y. Jeannin, A. Proust, F. Robert, *Angew. Chem.* **1989**, *101*, 1377; *Angew. Chem. Int. Ed. Engl.* **1989**, *28*, 1364.
[27] SHELX-PC Package, Bruker Analytical X-ray Systems, Madison, WI, **1998**.

Received: February 12, 2007
Published online: May 22, 2007

